International Journal of Wavelets, Multiresolution and Information Processing

SPECTRA AND FILTERING: A CLARIFICATION

Ch.-H. BRUNEAU

I.M.B, INRIA Team MC2, Université Bordeaux 1,*
351 Cours de la Libération, 33405 Talence Cedex, France
Charles-Henri.Bruneau@math.u-bordeaux1.fr

P. FISCHER

I.M.B., INRIA Team MC2, Université Bordeaux 1,
351 Cours de la Libération, 33405 Talence Cedex, France
Patrick.Fischer@math.u-bordeaux1.fr

Received (Day Month Year)
Revised (Day Month Year)
Communicated by (xxxxxxxxxx)

Filtering methods have been introduced in the early nineties, in 1988 by Farge *et al.* for a wavelet filtering, in 1987 by Benzi *et al.* and in 1994 by Borue for a direct cut-off filtering. The aim of these methods is to filter the velocity and/or the vorticity fields of two-dimensional turbulence experiments in order to enhance the various components of the fluid. Using this king of methods allows us to separate the vortices from the background essentially composed by vorticity filaments. We have also shown the ability of the wavelet packets in performing this filtering. However, we had underestimated, like Borue in 1994, the influence of the filtering process in the computation of the energy and/or enstrophy spectra. We will show in the present paper how the introduction of discontinuities due to the filtering process can subsequently modify the spectra.

Keywords: Wavelet packet; filtering methods; two dimensional turbulence.

AMS Subject Classification: 65T60, 60G35,76F65

1. Introduction

The results presented in Ref. 7, 8 and in Ref. 10 show that the wavelet packet decomposition is an adapted tool for studying two-dimensional turbulence. It is able to separate two type of structures, the vortices from the vorticity filaments. Spirals on top of the vortices have been also clearly observed. These spiral structures had been previously predicted by Vassilicos and Hunt [18]. Due to analysis errors in Ref. 10, the vorticity filaments had lead to an energy spectrum with a slope of about -5/3 and the vortices to an energy spectrum with a slope of -3. The inertial ranges where the scale laws had been observed seem to lie down on both sides, upscale and

*Institut de Mathématiques de Bordeaux

downscale, of the injection scale.
However, we didn't pay enough attention to the discontinuities that could be introduced by the filtering method. And this is particularly true for the direct filtering proposed by Benzi, Patarnello and Santangello [1,2] and later developed by Borue [3]. We will show in this paper that the -5/3 slope located in the end of the energy spectrum of the vorticity filaments is essentially due to the discontinuities. The spectra corresponding to the vortices are also polluted by spurious coefficients in Fourier space. This paper can be considered as a complement of Ref. 4 and Ref. 5 where several numerical methods for the computation of energy spectra were compared. These three papers show the influence of the numerical methods when computing spectra.
The first section of the paper is aimed to remind some technical details in the computation of energy spectra that are often forgotten in papers about two-dimensional turbulence.
In the second section, windowing methods for the computation of spectra in non-periodic domains are described. And finally, numerical results showing the effects of the filtering process are given and commented in the third section.

2. The energy and enstrophy spectra computations

First of all, we would like to point out some details rarely discussed in papers about two-dimensional turbulence. A more general and complete description of the theory can be found in Ref. 11 and Ref. 16.
The first point concerns the definition of the mean energy: mean energy *per unit mass* or mean energy *per unit wavenumber* ? The difference between the two definitions is small but can lead to some confusion.
The second point discussed in this part is about the relation between the energy and the enstrophy spectra. It is commonly admitted that the enstrophy spectrum $Z(k)$ is equal to k^2 times the energy spectrum $E(k)$. This equality is very important when studying the existence of dominant and subleading cascades in two-dimensional turbulence, as discussed in Ref. 17. However, it is not always true, and it will be shown in the sequel that our numerical experiments do not verify this equality.
The energy balance in Fourier space is obtained by applying a Fourier Transform to the corresponding energy balance in physical space:

$$\partial_t E(\boldsymbol{\xi}) = T(\boldsymbol{\xi}) + D(\boldsymbol{\xi})E(\boldsymbol{\xi}) + F(\boldsymbol{\xi}). \tag{2.1}$$

Here $\boldsymbol{\xi} = (\xi_x, \xi_y)$ is the Fourier variable in Fourier space, E the energy, T the non linear energy transfer, D the dissipation operator and F stands for the energy injection. In our experiments in the sequel, there won't be any 'artificial' injection since the turbulence will be naturally generated by obstacles.
One can then define the mean energy *per unit wavenumber* E_w as,

$$E_w \equiv \left\langle \frac{1}{2}|\hat{v}|^2 \right\rangle = \frac{1}{2}\frac{1}{S(Q)}\int_Q |\hat{v}(\boldsymbol{\xi})|^2 d\boldsymbol{\xi} \tag{2.2}$$

where Q denotes the square domain of definition of $\hat{v}$ (whose the maximum length is related to the discretization step size of the numerical computation according to the Shannon theorem) and $S(Q)$ its corresponding surface. This mean energy can be easily approximated in polar coordinates:

$$E_w \approx \frac{1}{2}\frac{1}{S(B_R)}\int_0^{2\pi}\int_0^R |\hat{v}(r,\theta)|^2 r dr d\theta \tag{2.3}$$

where B_R is the biggest circular domain of radius R included in Q. This last equation is not an exact formula since the corners of Q, where the values of $|\hat{v}|$ are very small, have been neglected. Considering the fact we are performing numerical computations on a discrete grid, on can define the discrete power spectral density function $E(k)$ by

$$E_w(k) = \frac{1}{2}\frac{1}{S_k}\int_0^{2\pi}\int_{k-1/2}^{k+1/2} |\hat{v}(r,\theta)|^2 r dr d\theta \quad \forall k > 0 \tag{2.4}$$

$$E_w(0) = \frac{1}{2}\frac{1}{S_0}\int_0^{2\pi}\int_0^{1/2} |\hat{v}(r,\theta)|^2 r dr d\theta. \tag{2.5}$$

with $S_k = 2\pi k$ the surface of the annulus centered around the integer $k = |\boldsymbol{k}|$, and $S_0 = \frac{\pi}{4}$ the surface of the circle of radius 1/2. In the same way, one can define the mean cumulative energy $\mathcal{E}_w^K$:

$$\mathcal{E}_w^K = \frac{1}{2}\frac{1}{S_K}\int_0^{2\pi}\int_0^{K} |\hat{v}(r,\theta)|^2 r dr d\theta. \tag{2.6}$$

with $S_K = \pi K^2$. One has to specify that the mean cumulative energy per unit wavenumber is not equal to the sum of the values of the mean energy spectrum since we are dealing with averages in both cases. The isotropic assumption allows for dependence only on the magnitude of the wavenumber and permits to neglect the angular dependence of $\hat{v}(r,\theta)$. This definition of the mean energy has been sometimes used but does not correspond to the most largely used definition by people studying two-dimensional turbulence. The usual mean energy is the mean energy *per unit mass* E and is defined by,

$$E \equiv \left\langle \frac{1}{2}|v|^2 \right\rangle = \frac{1}{2}\frac{1}{S(B_L)}\int_{B_L} |v(\boldsymbol{x})|^2 d\boldsymbol{x} \tag{2.7}$$

where B_L denotes the physical domain of definition of v and $S(B_L)$ its corresponding surface. If one considers now v as a L-periodic function, it can be decomposed as a Fourier series:

$$v(\boldsymbol{x}) = \sum_{\boldsymbol{k}} \hat{v}(\boldsymbol{k}) e^{\frac{2i\pi}{L}\boldsymbol{k}.\boldsymbol{x}}, \quad \boldsymbol{k} \in \mathbb{Z}^2. \tag{2.8}$$

The low-pass filtered velocity function is then defined as,

$$v_K^<(\boldsymbol{x}) = \sum_{|\boldsymbol{k}|\leq K} \hat{v}(\boldsymbol{k}) e^{\frac{2i\pi}{L}\boldsymbol{k}.\boldsymbol{x}} \tag{2.9}$$

and the high-pass filtered velocity function as:

$$v_K^>(\boldsymbol{x}) = \sum_{|\boldsymbol{k}|>K} \hat{v}(\boldsymbol{k}) e^{\frac{2i\pi}{L}\boldsymbol{k}.\boldsymbol{x}}. \tag{2.10}$$

This decomposition of the velocity,

$$v(\boldsymbol{x}) = v_K^<(\boldsymbol{x}) + v_K^>(\boldsymbol{x}), \tag{2.11}$$

was used for the first time by Obukhov [12,13]. Introducing this splitting in the Navier-Stokes equations, one obtain the scale-by-scale energy budget equation described by Frisch [11]:

$$\partial_t \mathcal{E}(K) + \Pi(K) = \mathcal{D}(K) + \mathcal{F}(K). \tag{2.12}$$

where

$$\mathcal{E}(K) \equiv \left\langle \frac{1}{2}|v_K^<|^2 \right\rangle = \frac{1}{2} \sum_{|\boldsymbol{k}|\leq K} |\hat{v}(\boldsymbol{k})|^2, \tag{2.13}$$

denotes the cumulative energy between wavenumber 0 and K, $\Pi(K)$ the energy flux through wavenumber K, $\mathcal{D}(K)$ the cumulative energy dissipation, and $\mathcal{F}(K)$ the cumulative energy injection. The energy spectrum is then defined by:

$$E(k) \equiv \frac{d\mathcal{E}(k)}{dk}. \tag{2.14}$$

Finally, both definitions for the mean energy spectrum are then linked to each other by:

$$E(k) = 2\pi k E_w(k). \tag{2.15}$$

Two-dimensional turbulence, in infinite or periodic domains, is governed by two invariants, the total energy:

$$E = \int_0^\infty E(k)dk, \tag{2.16}$$

and the total enstrophy,

$$Z = \int_0^\infty Z(k)dk, \tag{2.17}$$

where $Z(k)$ stands for the enstrophy spectrum.
The total enstrophy Z can be defined in the same way as the total energy,

$$Z \equiv \left\langle \frac{1}{2}|\boldsymbol{\omega}|^2 \right\rangle = \frac{1}{2}\frac{1}{S(B_L)} \int_{B_L} |\boldsymbol{\omega}(\boldsymbol{x})|^2 d\boldsymbol{x}, \tag{2.18}$$

where

$$\boldsymbol{\omega} = \boldsymbol{\nabla} \times \mathbf{u} \tag{2.19}$$

is the vorticity field. Because of equation (2.19), the energy and enstrophy spectra are linked to each other in Fourier space by the following relation:

$$Z(k) = \left(\frac{2\pi k}{L}\right)^2 E(k) \tag{2.20}$$

which reduces to

$$Z(k) = k^2 E(k) \tag{2.21}$$

in a 2π-periodic bounded domain. But, as described in Ref. 6, 10 and in the following section, we do not have any periodic boundary conditions in our numerical experiments, and the relation described above between the energy and the enstrophy spectra does not hold anymore. It will be shown in the sequel how the energy-enstrophy relation numerically diverges in our particular case.

3. Experimental setup

The experiment consists in the numerical simulation of a two dimensional channel, in which a vertical array of cylinders perturbs the flow. Along the sides of the channel, nine cylinders are placed horizontally to reinforce the injection scale. The two dimensional Navier Stokes equations are then solved numerically in a domain whose the length is four times the width $L = 1$. The Reynolds number based on the cylinders diameter (equal to $0.05 \times L$) is $Re = 50000$. The equations are solved in primitive variables with a multigrid procedure on a Cartesian mesh. A penalisation method is used to take into account the obstacles and a non reflecting boundary condition is set on the exit section of the channel to convey properly the vortices downstream. A Poiseuille flow is given upstream and the no-slip boundary condition is set on the walls of the channel. The discretization is done by a global second order scheme in time and space including an accurate third order approximation of convection terms.
A snapshot of the vorticity field is given in Figure 1, where one can see the three arrays of cylinders.

If one computes the energy and enstrophy spectra in the selected square of size $L = 1$ located at the end of the channel, one can check the validity of the relation (2.20) which writes,

$$Z(k) = 4\pi^2 k^2 E(k) \tag{3.1}$$

in our case.

The computations have been performed for ten different vorticity and velocity fields computed on a 2560×640 grid. The results are shown in Figure 2. It can be noticed that the relation (2.20) is more or less verified in a range laid from $k = 2$ to $k = 30 - 40$. This phenomenon has been statistically verified by computing the mean of the ratio $Z(k)/E(k)$ on 80 snapshots (computed on a 1280×320 grid).

The cutting process for selecting the square creates many discontinuities in the velocity and vorticity fields thus introducing essentially high frequency coefficients

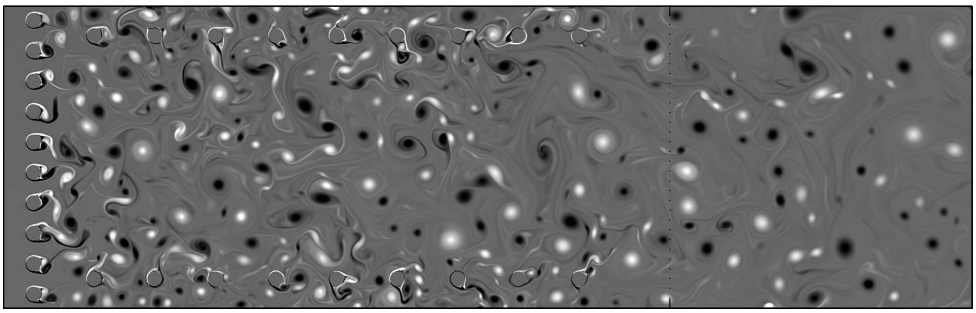

Fig. 1. Snapshot of the vorticity field

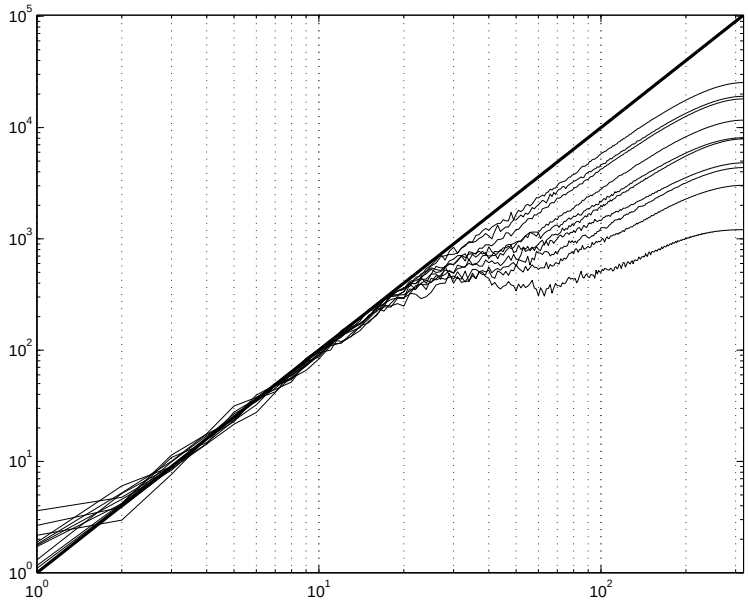

Fig. 2. $Z(k)/(4\pi^2 E(k))$ for 10 various snapshots.

in Fourier space. This phenomenon, well known from people using the classical FFT algorithm, is described in Ref. 14 and Ref. 15 but its negative consequence for interpretating the two-dimensional turbulence spectra has never been enlightened. One can avoid this problem by using a Windowed Fourier Transform. Different kind of windows can be used for that purpose. Several one-dimensional windows are shown in Figure 3.

The Tukey windows use a parameter allowing to vary the size of the horizontal plateau; 0.5 and 0.1 in the samples shown in this figure. All of these windows remove

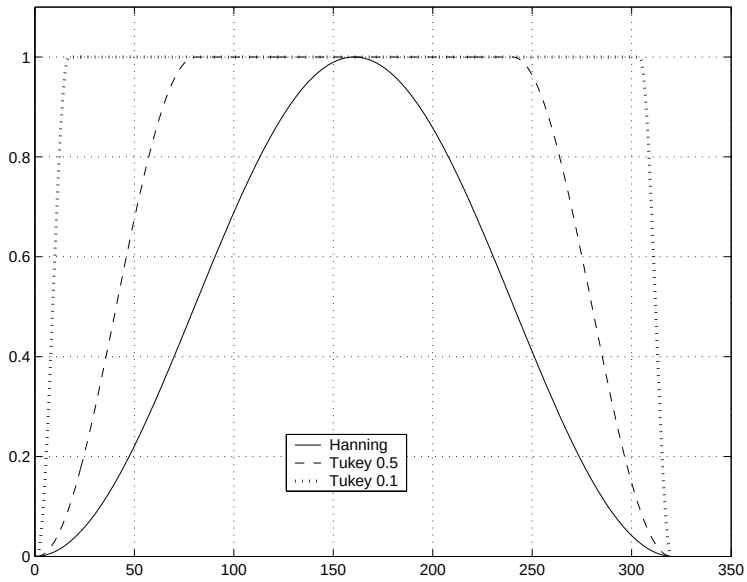

Fig. 3. Sample of several windows.

the Fourier coefficients created by the discontinuities but some of them, as the Hann window frequently called the Hanning window and often used in energy spectrum computations, also remove a significant part of the energy and enstrophy contained in the fields. The resulting energy spectra computed using these windows are shown in Figure 4.

It can be noticed that the slope detected between $k = 15$ and $k = 60$ is always around $k^{-5.5}$ whatever the choice of the window is. If one use a window with a larger plateau, Tukey with the parameter equal to 0.02 for instance, the smoothing of the discontinuities is less efficient and the spectrum is closer to the non-windowed spectrum.

The efficiency of the windowing process is clearly demonstrated in Figure 4. The best window being the one allowing to smooth the discontinuities without removing the global frequency contents.

According to that study, one can conclude that the often used Hann window removes a non negligible part of the energy. The window which seems to realize the best compromise between smoothing the discontinuities and removing the energy contents is the Tukey window with a parameter around 0.1. The effects of the windowing can be also visualized in Figure 5 which represents the windowed average ratio $Z(k)/E(k)$. The curve for the Hann windowing has not been reproduced in Figure 5 since it was exactly the same as for the Tukey (0.5) windowing.

A normalization based on the l^2 norm of the window function is often used to

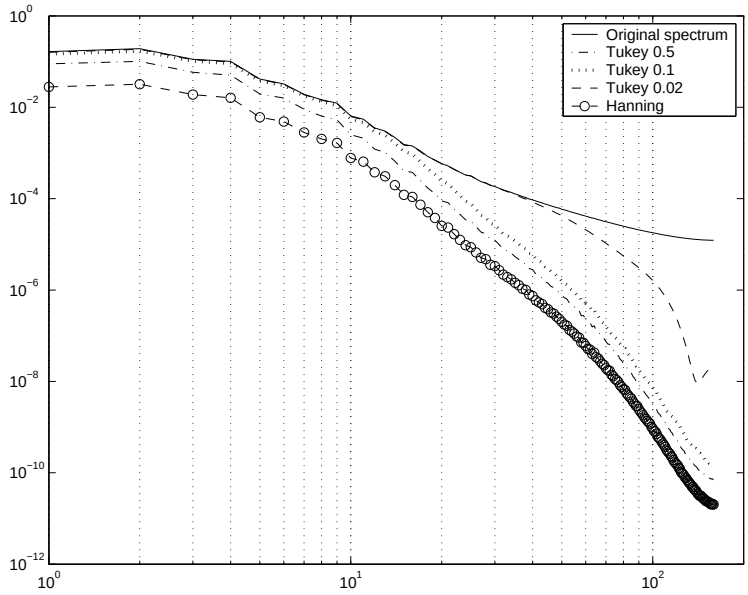

Fig. 4. Various windowed energy spectra.

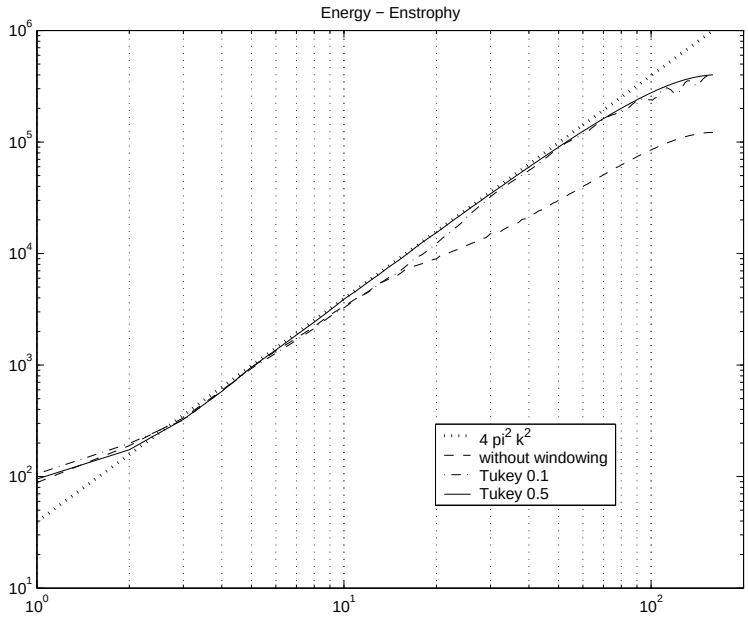

Fig. 5. Windowed average $Z(k)/E(k)$.

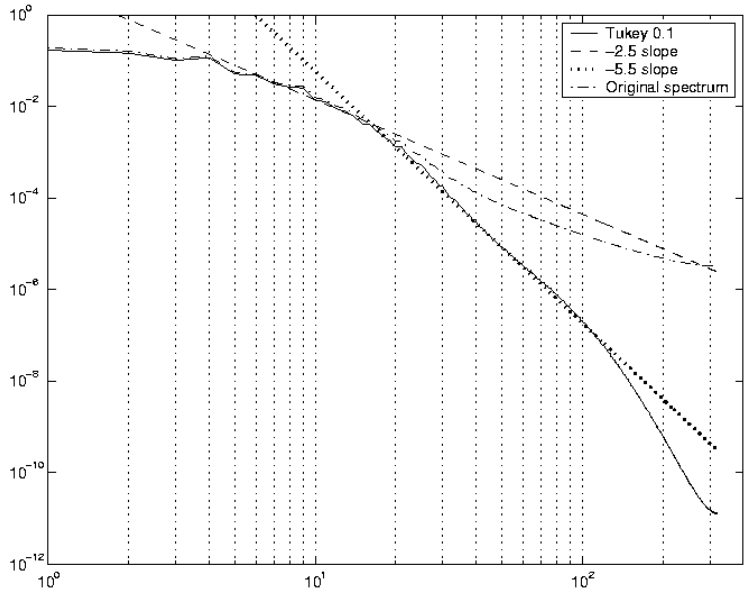

Fig. 6. Energy spectra computed with and without a Tukey (0.1) window on a 2560×640 fine grid.

artificially reinject the energy removed by the windowing process. See for instance Ref. 14. This trick can be partially acceptable when one considers only the shape of the spectra, but cannot be considered when one is interested in studying energy and/or enstrophy fluxes. It is then essential to assess the original physical contents. All these results show that one should be very careful when computing energy and/or enstrophy spectra. A large part of the spectra can be "polluted" by spurious coefficients created by the computing method itself. This phenomenon is not due to the size of the discretization grid, and has been also verified on a 2560×640 grid. The same averages computed with 25 snapshots are shown in Figures 6 and 7.

One can see from this first study that the representation of discontinuities in Fourier space can alter the spectra by generating many spurious coefficients not linked to the real frequency contents.

4. The filtering algorithm and its use

We have seen in the previous section the effects of the discontinuities created by the selection of a square within a velocity or vorticity field. Then one may wonder if the discontinuities created by a filtering process allowing to separate the vortices from the vorticity filaments can be responsible of the creation of the same kind of spurious coefficients in Fourier space. The goal of the present section is to show what is the real frequency contents in the filtered fields, and what is the part due

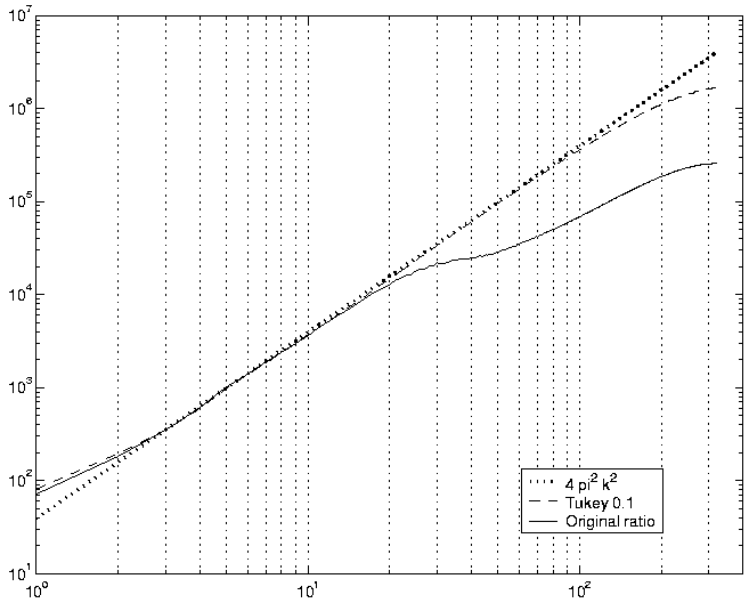

Fig. 7. $Z(k)/E(k)$ computed with and without a Tukey (0.1) window on a 2560×640 fine grid.

to the representation of the discontinuities. A cut-off filtering and a wavelet packet decomposition will be considered in the sequel. All the computations in this section have been performed using a 2560×640 grid.

4.1. *Cut-off filtering*

It is shown in Figures 8 and 9 the two cut-off filtered vorticity fields corresponding to the particular snapshot given in Figure 10.

One can see that the vortices are clearly extracted from the filaments. The vortices and the filaments fields, as described in Ref. 3, should lead to different energy spectra. The average energy spectra computed with 80 snapshots for the filtered fields are given in Figure 11. One should mentioned here that a windowed Fourier Transform with a Tukey (0.1) window has been used in order to remove the spurious coefficients generated by the boundary conditions.

As expected, the spectrum of the fields with only the vortices does not present the same decrease as the spectrum of the filaments fields. Slope around -3 are observed for the vortices, and around $-5/3$ for the filaments. The theoretical value of $-5/3$ has been explained by Vassilicos and Hunt, and numerically observed by Borue. However, if one carefully observes the spectra, one can notice that both fields have the same behavior from $k \approx 20$ to the end of the spectra. This range is exactly the same as the one enlightened in the previous section. The slopes observed in this range are also due to discontinuities, but created by the filtering process instead of

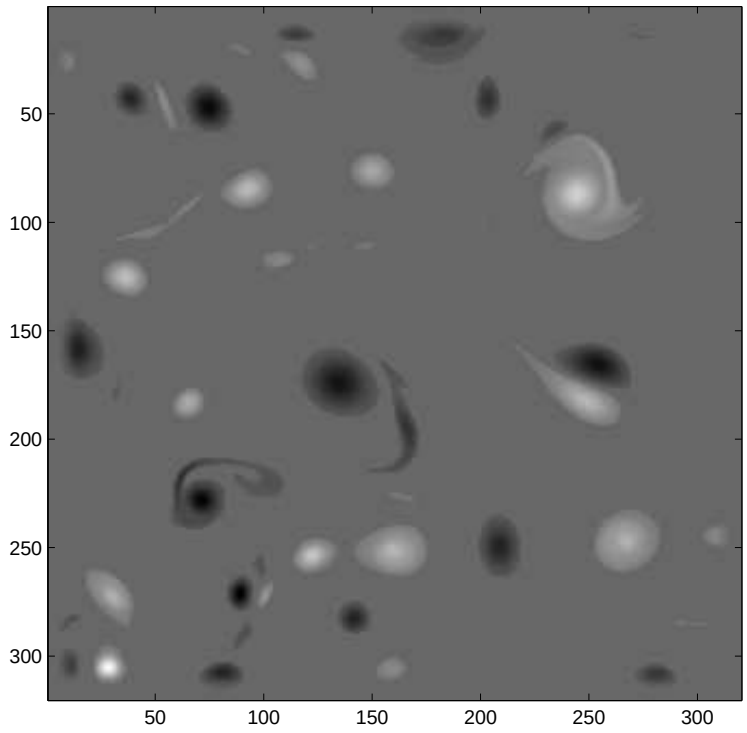

Fig. 8. Vortices obtained thanks to a cut-off filtering.

the boundary cutting. Only the effects of the discontinuities created by the filtering inside the domain are observed here. It's not surprising that both fields present the same behavior in this spectral range since the discontinuities are the same in both filtered fields. In order to have a better understanding of the phenomenon, we propose to study the problem on a one-dimensional cut of the field. Let's take for instance a one-dimensional cut located along the row 250 of the vortices field in Figure 8. The one-dimensional curve is given in Figure 12.

This cut contains four vortices, and the corresponding one-dimensional Fourier spectrum is given in Figure 13.

This spectrum is obviously very noisy since it has been computed with only one-dimensional signal. Now, we are going to analyze a Gaussian fitting of the same signal. As can be verified in Figure 12, the Gaussian fitting is really a continuous version of our original cut.

The main difference between these two curves is the smoothing process of the discontinuities. One can compare the spectrum of the Gaussian fit to the spectrum of the original cut previously computed and represented in Figure 13.

As can be easily observed, both spectra are identical in the beginning of the frequency range and differ only from $k \approx 20$, where the continuous approximation

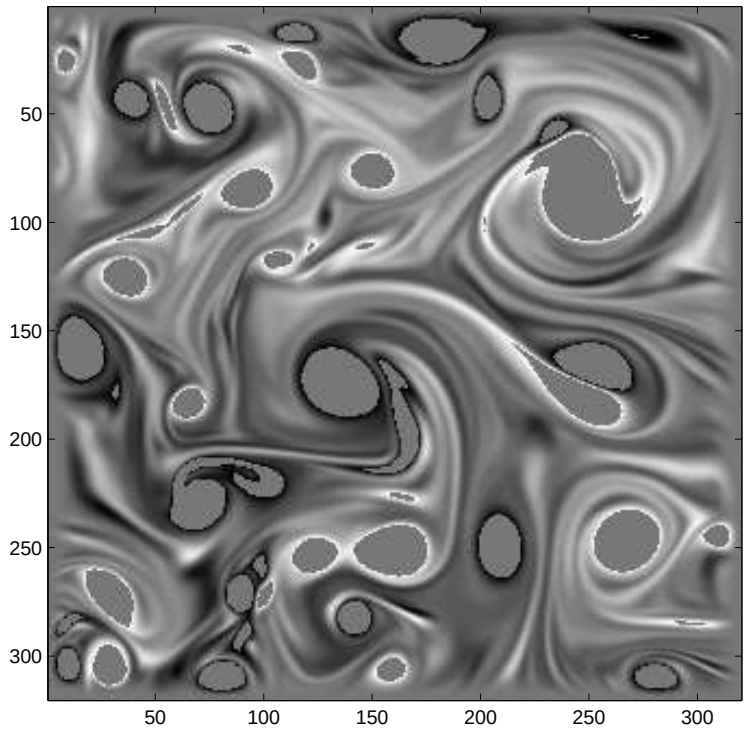

Fig. 9. Vorticity filaments obtained thanks to a cut-off filtering.

spectrum presents a very fast decay to zero. The conclusion is that many spurious coefficients created by the discontinuities are hiding the real spectral behavior in the range from $k \approx 20$ to the finest scale allowed by the discretization step size.
Why is it so important to mention that ? Because in our numerical experiments, the injection scale given by the cylinders diameter is precisely that value, and then the hypothetical enstrophy cascade described by the theory would be completely hidden by spurious Fourier coefficients.
The same phenomenon obviously occurs during the computation of two-dimensional spectra of filtered fields. Then an interesting solution to avoid this problem consists in using a smooth filtering like the wavelet decomposition.

4.2. *Wavelet packet filtering*

The theory concerning the wavelet packets has been already detailed in Ref. 10 and won't be reminded here. The same Daubechies type wavelets are used in the current paper to build the packets array, and the entropy criterion is used in the best basis selection process. In Ref. 10, few tests had been performed in order to get the best wavelet mother, and to determine how many scales would be necessary to get an efficient representation of the flow. The criterion was then the minimization

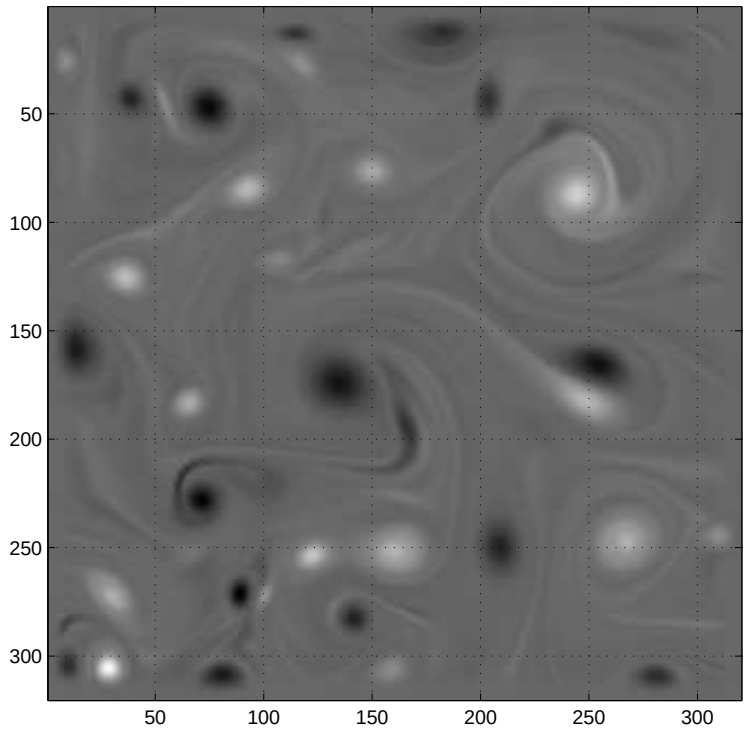

Fig. 10. Snapshot of the vorticity field.

of the entropy. It had been shown that it was not necessary to perform the wavelet packet decomposition over more than 3 scales when the finest scale corresponds to a 1280×320 grid. It has to be reminded that the scale sequence goes from finest scales to coarsest scales. It leads to the most efficient representation in the entropy meaning but not to the smoothest fields after filtering. The two goals being completely different.

In order to evaluate the importance of the decomposition depth for the discontinuities smoothing, one will compare the cut-off filtering to wavelet packet filtering performed over 1, 2, 3 and 4 scales. It will be shown that, as long as one is concerned with smoothing the discontinuities, it is necessary to go over at least 4 scales (for a finest scale corresponding to a 1280×320 grid). That means that in Ref. 10, where only 3 scales were considered, some spurious coefficients due to the discontinuities remained in the spectra. This problem has to be particularly taken into account since it could lead to a misinterpretation of the results. If one observes for instance the spectrum of the vorticity filaments field in Figure 14, the spurious coefficients are exactly in the continuation of a $k^{-5/3}$ slope. The misinterpretation would be to think that there exists an inverse energy cascade over a longer range. However, that does not mean neither that an inverse energy cascade does not exist in that area....

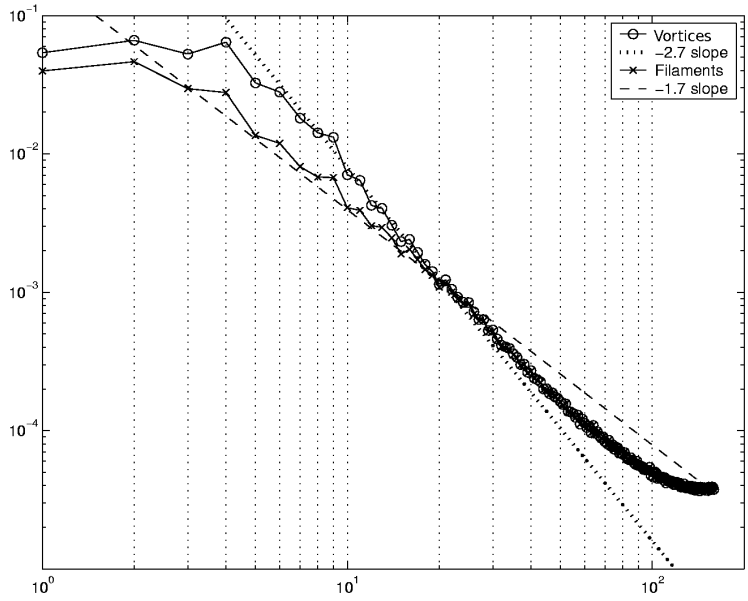

Fig. 11. Energy spectra obtained thanks to a cut-off filtering.

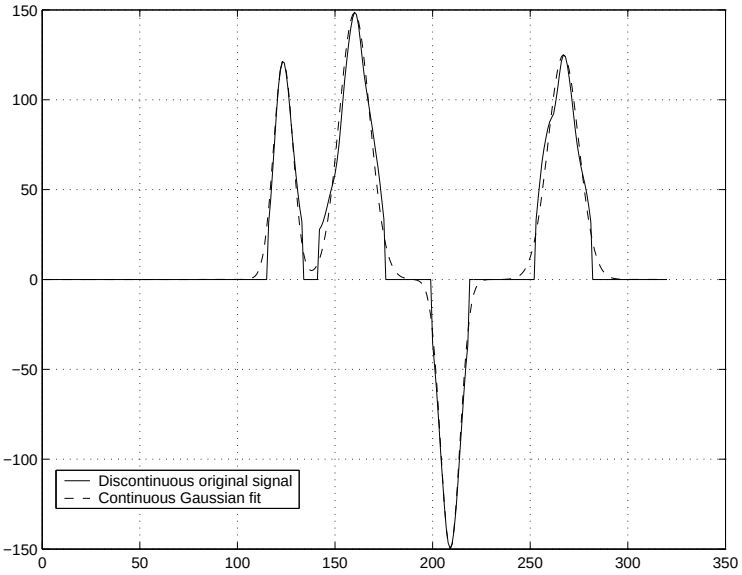

Fig. 12. Gaussian fit of the one-dimensional cut.

That just means that the end of the spectrum from $k \approx 20$ is mainly dominated by spurious coefficients created by the discontinuities, and so considerably alter the

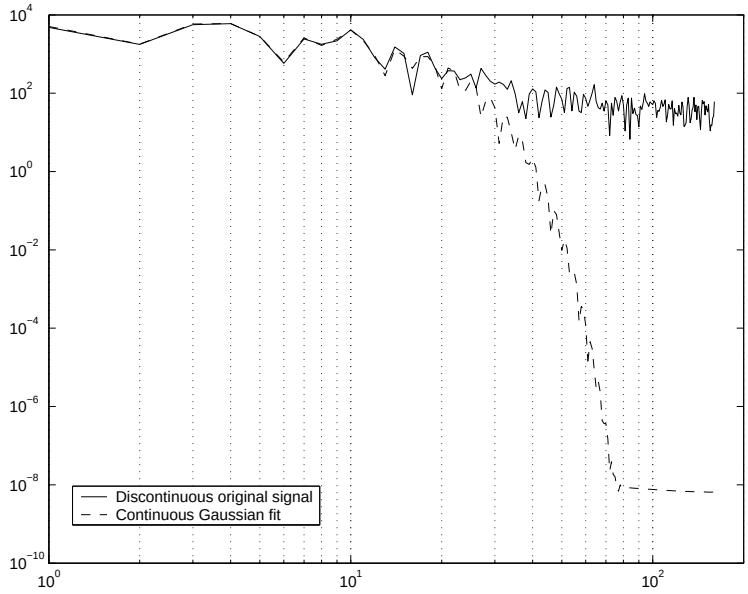

Fig. 13. One-dimensional cut spectra.

analysis of the physical contents. The same problem occurs obviously with the field containing the vortices in Figure 15.

However, when comparing Figure 14 to Figure 15, one can notice that the spectra in the first part of the spectra (i.e. from $k = 1$ to $k \approx 15$) in Figure 15 are closer to each other than in Figure 14. The difference between the cut-off filtering and the 4 scales wavelet packet filtering in Figure 14 is not due to the discontinuities, otherwise it would be also observed in Figure 15. It is due to the creation of new structures or rather to the creation of non-structures of the same size as the vortices. When observing the Figure 9, one can immediately remark the location of the would-be vortices. These patterns are obviously detected by the Fourier transform and can be found in the large scales range of the energy spectrum. This phenomenon does not occur for the vortices field, as can be checked in Figure 15, since the patterns do really exist. One can also verify that these patterns do not exist with a smooth wavelet packet filtering. The filtered vorticity fields obtained thanks to a 4 scales wavelet packet filtering are given in Figures 16 and 17. The patterns due to the extraction of the vortices have disappeared and have been replaced by the spiral structures predicted in Ref. 18 to give a continuous field of vorticity filaments.

The spectra corresponding to the original and filtered fields computed over 4 scales are given in Figure 18.

One can notice that the initial spectrum can be exactly decomposed as the sum of the two filtered spectra and the $k^{-5/3}$ slope previously detected in the filaments spectrum is not observed anymore and has been replaced by a scaling in $\approx k^{-5}$.

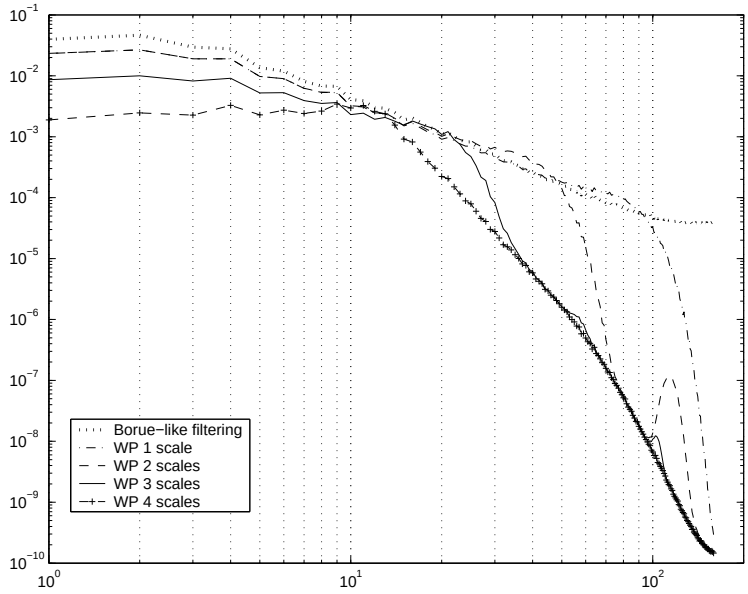

Fig. 14. Filtered energy spectra of the filaments.

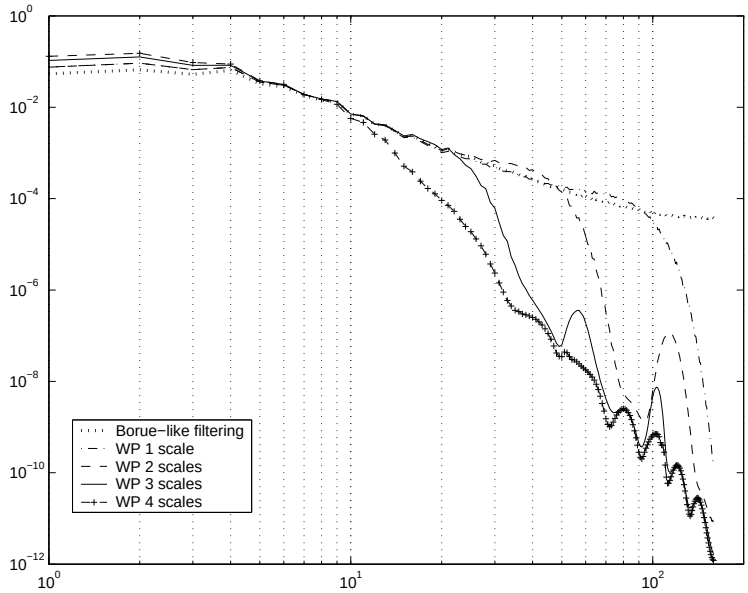

Fig. 15. Filtered energy spectra of the vortices.

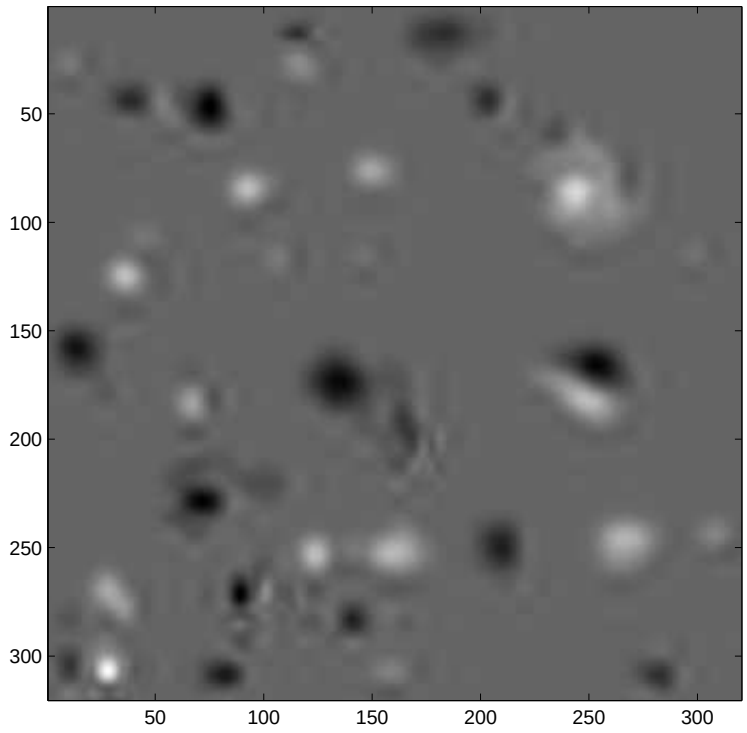

Fig. 16. Vortices obtained thanks to a 4 scales wavelet packet filtering.

Thus the spurious coefficients created in Fourier space by the discontinuities had lead to an erroneous analysis of the physical phenomena.

5. Conclusion

This paper mainly points out two technical pitfalls when computing energy or enstrophy spectra and filtering velocity or vorticity fields. These pitfalls can lead to a misinterpretation in the analysis of the spectrum physical contents. When studying a physical phenomenon, one should never forget that the choice of the observation tool is never trivial and can alter the results. Of course the above discussion does not affect the results of the literature in the periodic case or in the non-periodic case when a window is properly used but could affect some results obtained with a discontinuous filtering.

Acknowledgments

The authors acknowledge with appreciation Hamid Kellay for stimulating discussions and useful comments.

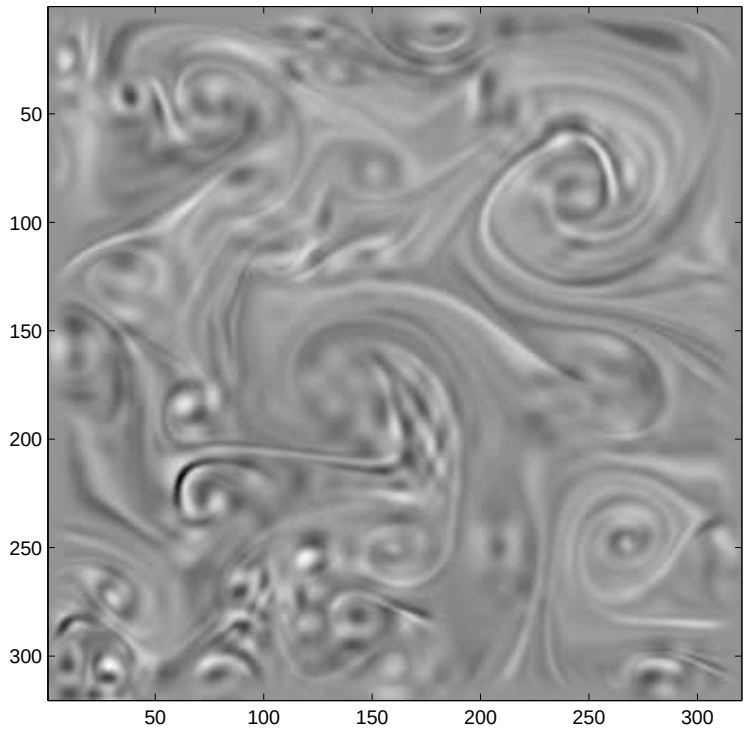

Fig. 17. Vorticity filaments and spirals obtained thanks to a 4 scales wavelet packet filtering.

References

1. R. Benzi, S. Patarnello, P. Santangelo, On the statistical properties of two-dimensional decaying turbulence, *Europhys. Lett.* **3** (1987) 811–818.
2. R. Benzi, S. Patarnello, P. Santangelo, Self-similar coherent structures in two-dimensional decaying turbulence, *J. Phys. A: Math. Gen.* **21** (1988) 1221–1237.
3. V. Borue, Inverse energy cascade in stationary two-dimensional homogeneous turbulence, *Phys. Rev. Lett.* **72** (1994) 1475–1478.
4. Ch. H. Bruneau, P. Fischer, Z. Peter, A. Yger, Comparison of Numerical Methods for the Computation of Energy Spectra in 2D Turbulence. Part I: Direct methods, *Sampl. Theory Signal Image Process.* **4** (2005) 169–192.
5. Ch. H. Bruneau, P. Fischer, Z. Peter, A. Yger, Comparison of Numerical Methods for the Computation of Energy Spectra in 2D Turbulence. Part II: Adaptative Algorithms, *Sampl. Theory Signal Image Process.* **4** (2005) 271–280.
6. Ch. H. Bruneau, H. Kellay, Experiments and numerical simulations of two-dimensional turbulence, *Phys. Rev. E* **71** (2005) 046305.
7. M. Farge, G. Rabreau, Wavelet transform to detect and analyze coherent structures in two-dimensional turbulent flows, *C. R. Acad. Sci. Paris* **t. 307, Srie II** (1988) 1479–1486.
8. M. Farge, N. Kevlahan, Vorticity filaments in two-dimensional turbulence: creation, stability and effect, *J. Fluid Mech.* **346** (1997) 49–76.
9. M. Farge, K. Schneider, N. Kevlahan, Non-Gaussianity and coherent vortex simulation

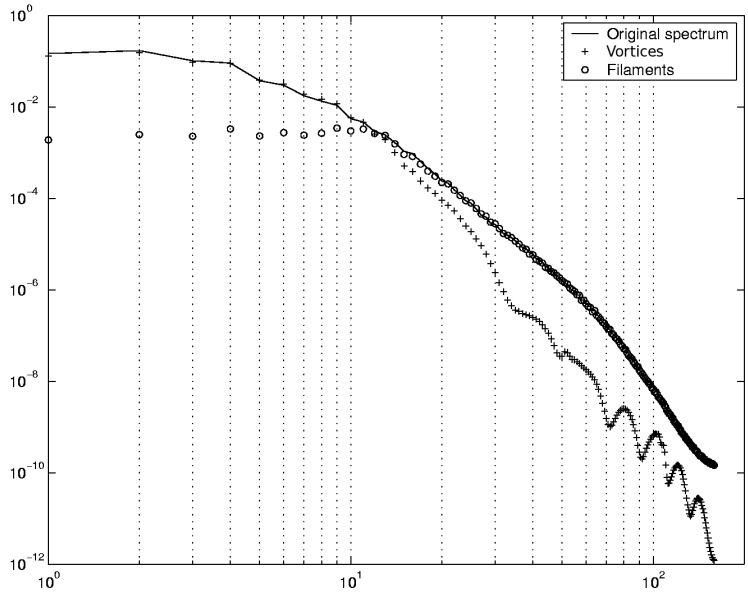

Fig. 18. Original and filtered (wavelet packets with 4 scales) energy spectra .

for two-dimensional turbulence using an adaptative orthogonal wavelet basis, *Physics of Fluids* **11** (1999) 2187–2201.

10. P. Fischer Multiresolution analysis for two-dimensional turbulence. Part 1: Wavelets vs Cosine packets, a comparative study, *Discrete and Continuous Dynamical Systems B* **5** (2005) 659–686.
11. U. Frisch, *Turbulence: The legacy of A. N. Kolmogorov* (Cambridge University Press, Cambridge, 1995) .
12. A. M. Obukhov, On the distribution of energy in the spectrum of turbulent flow, *Dokl. Akad. Nauk SSSR* **32** (1941) 22–24.
13. A. M. Obukhov, Spectral energy disctribution in a turbulent flow, *Izv. Akad. Nauk SSSR Ser. Geogr. Geofiz.* **5** (1941) 453–466.
14. W. Press, S. Teukolsky, W. Vetterling, B. Flannery, *Numerical Recipes* (Cambridge University Press, Cambridge, 2001).
15. M. Priestley *Spectral Analysis and Time Series* (Academic Press, 1981).
16. P. Tabeling, Two-dimensional turbulence: a physicist approach, *Phys. Rep.* **362** (2002) 1–62.
17. K.K. Tung, E. Gkioulekas, Does the subdominant part of the energy spectrum due to downscale energy cascade remain hidden in quasi-geostrophic turbulence?, submitted to *J. Atmos. Sci.*
18. J.C. Vassilicos, J.C. Hunt, Fractal dimensions and spectra of interfaces with application to turbulence, *Proc. R. Soc. Lond.* **A 435** (1991) 505–534.